Dental evidence for ontogenetic differences between modern humans and Neanderthals

Tanya M. Smith[a,b,1], Paul Tafforeau[c,1], Donald J. Reid[d], Joane Pouech[b,c], Vincent Lazzari[b,c,e], John P. Zermeno[a], Debbie Guatelli-Steinberg[f], Anthony J. Olejniczak[b], Almut Hoffman[g], Jakov Radovčić[h], Masrour Makaremi[i], Michel Toussaint[j], Chris Stringer[k], and Jean-Jacques Hublin[b]

[a]Department of Human Evolutionary Biology, Harvard University, Cambridge, MA 02138; [b]Department of Human Evolution, Max Planck Institute for Evolutionary Anthropology, 04103 Leipzig, Germany; [c]European Synchrotron Radiation Facility, BP 220, 38046 Grenoble Cedex, France; [d]Department of Oral Biology, School of Dental Sciences, Newcastle University, Newcastle upon Tyne NE2 4BW, United Kingdom; [e]International Institute of Paleoprimatology and Human Paleontology: Evolution and Paleoenvironments, Unité Mixte de Recherche Centre National de la Recherche Scientifique 6046, Université de Poitiers, 86022 Poitiers cedex, France; [f]Department of Anthropology, Ohio State University, Columbus, OH 43210; [g]Museum für Vor- und Frühgeschichte, Schloss Charlottenburg–Langhansbau, D-14059 Berlin, Germany; [h]Croatian Natural History Museum, 10000 Zagreb, Croatia; [i]Department of Orthodontics, University of Bordeaux II, 33000 Bordeaux, France; [j]Direction de l'Archeologie, Service Public de Wallonie, 5100 Namur, Belgium; and [k]Department of Palaeontology, Natural History Museum, London SW7 5BD, United Kingdom

Edited* by Richard G. Klein, Stanford University, Stanford, CA, and approved October 17, 2010 (received for review July 26, 2010)

Humans have an unusual life history, with an early weaning age, long childhood, late first reproduction, short interbirth intervals, and long lifespan. In contrast, great apes wean later, reproduce earlier, and have longer intervals between births. Despite 80 y of speculation, the origins of these developmental patterns in *Homo sapiens* remain unknown. Because they record daily growth during formation, teeth provide important insights, revealing that australopithecines and early *Homo* had more rapid ontogenies than recent humans. Dental development in later *Homo* species has been intensely debated, most notably the issue of whether Neanderthals and *H. sapiens* differ. Here we apply synchrotron virtual histology to a geographically and temporally diverse sample of Middle Paleolithic juveniles, including Neanderthals, to assess tooth formation and calculate age at death from dental microstructure. We find that most Neanderthal tooth crowns grew more rapidly than modern human teeth, resulting in significantly faster dental maturation. In contrast, Middle Paleolithic *H. sapiens* juveniles show greater similarity to recent humans. These findings are consistent with recent cranial and molecular evidence for subtle developmental differences between Neanderthals and *H. sapiens*. When compared with earlier hominin taxa, both Neanderthals and *H. sapiens* have extended the duration of dental development. This period of dental immaturity is particularly prolonged in modern humans.

hominin ontogeny | human evolution | modern human origins | tooth growth | biological rhythm

Reconstructing the evolution of human development from a severely limited fossil record is a fundamental challenge (1). Dental remains have figured prominently in debates over hominin ontogeny for decades, as they are frequently recovered in fossil assemblages and represent a reliable index of maturity. Moreover, when considered across the Primate order, dental eruption ages are broadly correlated with several life history events (e.g., ages at weaning and first reproduction) and physical attributes (e.g., body and brain mass) (2, 3; but see refs. 4–7). Variation among primate life histories has primarily been ascribed to differential mortality rates, as well as ecological niches, lifestyles, social complexity, cognitive development, or a combination of these factors (4, 5, 8). Although is it well established that humans are developmentally unique among living primates (9), weaning earlier and reproducing later than expected, the adaptive significance and evolutionary origins of our prolonged childhood are unresolved (1, 9–11).

Tooth histology, involving quantification of microscopic growth, is the most effective means of determining developmental rates, eruption ages, and age at death in juvenile hominins (12–15). Studies of dental growth have revealed that Pliocene to Early Pleistocene hominin ontogeny was more rapid than that of recent humans (12, 16, 17), but data from limited Neanderthal samples continues to be vigorously debated (7, 13, 18). A paucity of information on dental development in hominins postdating *Homo erectus*, coupled with conflicting interpretations of Neanderthal ontogeny, complicates assessment of the modern human (fossil and recent *Homo sapiens*) and Neanderthal ancestral condition. To address these limitations, we apply synchrotron imaging to quantify dental development and age at death in the largest sample of Neanderthal and fossil *H. sapiens* juveniles studied to date (Fig. 1, Table 1, and Movie S1). Furthermore, we reevaluate results obtained from single juveniles of both taxa (13, 14) and contrast these expanded samples with radiographic and histological data from recent human populations. Although traditional histological methods are destructive, generally prohibiting comprehensive studies of rare fossil material, recent advances in synchrotron X-ray imaging now permit accurate 3D virtual histology (19, 20). This nondestructive method enables us to assess internal records of dental development in key hominin fossils spanning a range of ontogenetic stages, geographic sources, and geological ages.

Studies of hominin dental growth rely on the fact that tooth crowns and roots form through rhythmic cellular activation and secretion, producing a permanent record of mineralized growth layers in enamel and dentine (reviewed in ref. 15; explained further in *SI Appendix*). Importantly, counts and measurements of these progressive short- (daily) and long-period (> daily) increments yield rates of secretion and extension, allowing crown and root formation time estimation. Moreover, the remarkable production of a line coincident with birth in permanent first molars (M1s) allows developmental time to be registered with an individual's actual age. When this neonatal line can be identified and subsequent development assessed from enamel and dentine increments, age at death may be estimated to within 5% of an individual's true age (21–23). This histological approach is a substantial improvement over the nearly ubiquitous application of recent human or ape developmental standards to age juvenile

Author contributions: T.M.S. and J.-J.H. designed research; T.M.S., P.T., D.J.R., J.P., V.L., J.P.Z., and A.J.O. performed research; P.T., D.J.R., J.P.Z., D.G.-S., A.H., J.R., M.M., M.T., and C.S. contributed new reagents/analytic tools; T.M.S., P.T., D.J.R., J.P., and V.L. analyzed data; T.M.S., P.T., J.P., V.L., J.P.Z., and A.J.O collected virtual data; T.M.S. and D.J.R. collected additional data from casts and sections; D.G-S., A.H., J.R., M.M., M.T., C.S., and J-J.H provided assistance with data acquisition; and T.M.S., P.T., D.J.R., D.G.-S., A.J.O., and J.-J.H. wrote the paper.

The authors declare no conflict of interest.

*This Direct Submission article had a prearranged editor.

Freely available online through the PNAS open access option.

[1]To whom correspondence may be addressed. E-mail: tsmith@fas.harvard.edu or paul.tafforeau@esrf.fr.

This article contains supporting information online at www.pnas.org/lookup/suppl/doi:10.1073/pnas.1010906107/-/DCSupplemental.

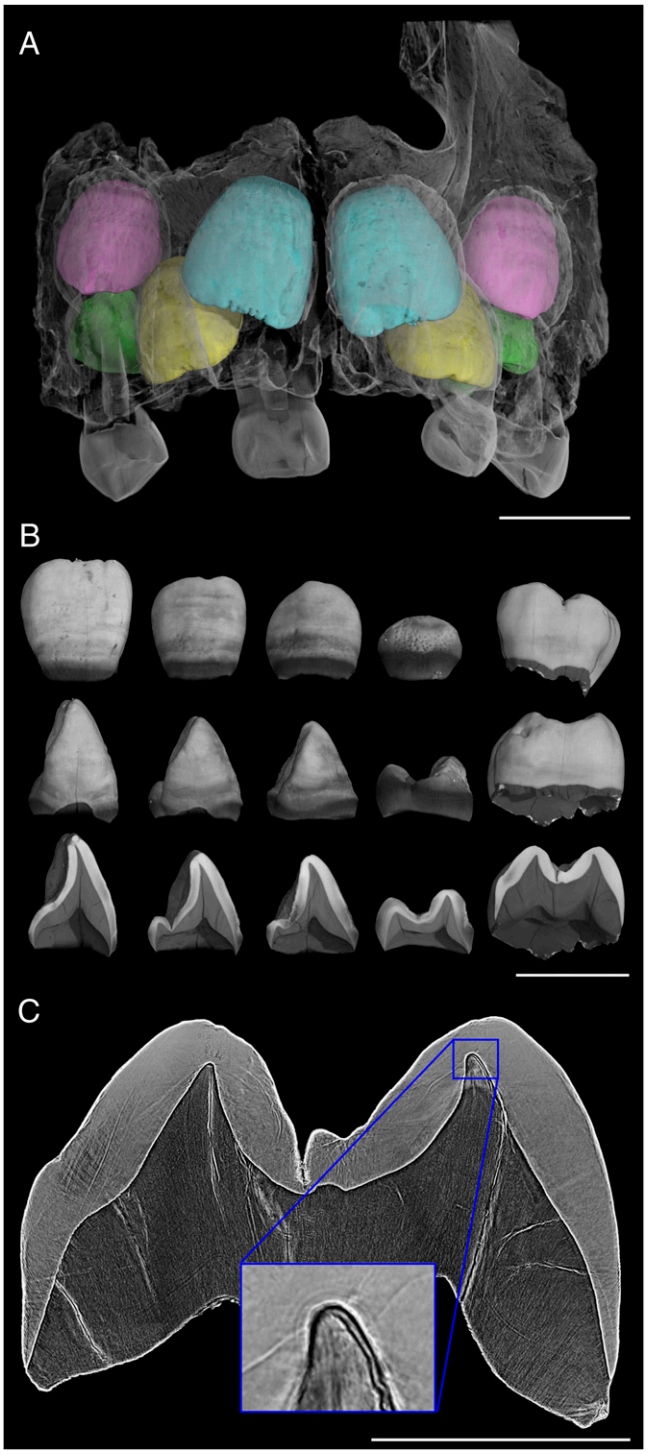

Fig. 1. Virtual histology of the maxillary dentition from the 3-y-old Engis 2 Neanderthal. (*A*) Synchrotron micro-CT scan (31.3-μm voxel size) showing central incisors in light blue, lateral incisors in yellow, canines in pink, and third premolars in green. (Deciduous elements are not rendered in color as they were not studied.) (*B*) Isolated elements and cross-sectional slices show the degree of permanent tooth calcification and broad horizontal hypoplastic bands. (Scale bars in *A* and *B*, 10 mm.) (*C*) Synchrotron phase contrast image (4.95-μm voxel size) used to count long-period lines in the maxillary first molar. (Scale bar, 5 mm.) (*Inset*) The neonatal line just above the conical dentine horn tip of the mesiobuccal cusp, estimated to have begun forming 17 d before birth.

hominins. Thus, independent chronologies can now be precisely developed from individuals who died while forming their dentitions, avoiding circular comparisons with living taxa, and permitting statistical assessment of ontogenetic variation.

Results and Discussion

To calculate crown formation time, molar eruption age, and age at death, we quantified the following standard developmental variables: cuspal enamel thickness, long-period line periodicity (number of daily increments between successive long-period lines), total number of long-period lines in enamel (Retzius lines or perikymata), and coronal extension rate (speed at which enamel-forming cells are activated to begin secretion along the enamel-dentine junction) in 90 permanent teeth from 28 Neanderthals and 39 permanent teeth from 9 fossil *H. sapiens* individuals (*Materials and Methods* and *SI Appendix*). These data were compared with 464 recent human teeth (> 300 individuals). This sample reveals that cuspal enamel is significantly thinner in Neanderthals than in recent humans for 10 of 14 tooth-specific comparisons (*SI Appendix*, Tables S1 and S2). Importantly, thinner cuspal enamel in Neanderthals formed over shorter periods than recent humans, as mean cuspal secretion rates are nearly identical in both taxa (12, 18, 24). Cuspal thickness in fossil *H. sapiens* is similar to that of recent humans, although certain postcanine teeth have thicker enamel in the fossil sample. The average Neanderthal long-period line periodicity is 7.4 d (range: 6–9; mode: 7–8; $n = 11$), which is significantly lower ($Z = -2.863$, $P < 0.01$) than in recent humans (mean: 8.3 d; mode: 8; range: 6–12; $n = 365$), but not statistically different from fossil *H. sapiens* (mean: 8.0 d; mode: 7–8; range: 7–10; $n = 5$) (*SI Appendix*, Table S3). Total numbers of Neanderthal long-period lines are similar to recent humans (*SI Appendix*, Table S4), as previously noted for a larger sample (25). Coronal extension rates are higher in Neanderthals (*SI Appendix*, Table S5), exceeding recent human ranges in 10 of 13 comparisons (Fig. 2). Thus, thinner enamel, lower long-period line periodicities, and faster extension rates result in lower crown formation times in Neanderthals than in recent humans (*SI Appendix*, Table S6). Crown formation times in fossil *H. sapiens* are more similar to recent humans than to Neanderthals, exceeding recent human values in some instances (14).

Combining histological data on initiation ages, crown formation times, and root formation times yields age-at-death estimates for six Neanderthal and two fossil *H. sapiens* juveniles (Table 1). To assess how these individuals compare with a recent human ontogenetic model, calcification stages of each tooth were scored (*Materials and Methods* and *SI Appendix*, Table S7), stages were converted to mean human ages (following ref. 26), and these ages were averaged across each dentition to yield age at death. Comparisons of our histologically determined ages with ages predicted from recent humans demonstrate that most of the Neanderthal dentitions we examined grew more rapidly than recent and fossil *H. sapiens* (Fig. 3). A significant difference ($L = 8.166$ at $\alpha = 0.05$) exists between the slopes of Neanderthal (1.41) and recent human (0.93) dental trajectories. Recent human dental standards overestimate age at death in several Neanderthals, but these same standards either accurately predict or underestimate age at death in living and fossil *H. sapiens*. Variation within formation times or the degree of dental precocity in Neanderthals does not appear to be related to ontogenetic stage, geological age, or geography, although both individuals from Belgian sites (Engis 2 and Scladina) show particularly rapid development. Thus, comparative ontogenetic studies should not use recent human dental standards to assign ages to juvenile Neanderthals.

When dentition-wide calcification patterns are compared further, rapid development in Neanderthals appears to primarily result from accelerated molar development (earlier age of completion, shorter duration of formation, and/or earlier initiation age). Recent human M1s initiate calcification 2 to 3 wk before

Table 1. Middle Paleolithic juvenile hominins included in the present study

Taxon	Fossil	Locality	Date, kya	Previous age, y	New age, y
Neanderthals	Engis 2	Engis, Belgium	>30–50	2–6	3.0
	Gibraltar 2	Devil's Tower, Gibraltar	30–50	3.1–5.8	4.6
	La Quina H18	La Quina, France	45–60	7	Unknown
	Krapina Maxilla B	Krapina, Croatia	100–127	6.5–8	5.9
	Obi-Rakhmat 1	Obi-Rakhmat, Uzbekistan	75	9–12	6.0–8.1
	Scladina	Scladina, Belgium	80–127	8.5–12	8.0
	Krapina Maxilla C	Krapina, Croatia	100–127	10–10.5	Unknown
	Le Moustier 1	Le Moustier, France	40	12–20	11.6–12.1
H. sapiens	Qafzeh 10	Qafzeh, Israel	90–100	6	5.1
	Qafzeh 15	Qafzeh, Israel	90–100	9	Unknown
	Irhoud 3	Irhoud, Morocco	160	7–8	7.8

Previous ages provided for historical reference only; most sources do not explain their method for determining age. New ages determined from tooth histology in this study.

birth, completing crown formation by about 3 y of age (27). Neanderthal M1 crowns also began forming 2 to 3 wk before birth (Fig. 1 and *SI Appendix*, Fig. S1), completing formation ≈6 mo earlier than recent humans (and thus beginning root initiation at younger ages). Although M1 initiation age appears to be fairly conserved across hominins, maxillary M3 initiation in the Scladina juvenile occurred at 5.9 y (13), which is 2 to 4 y earlier than average mandibular M3 initiation ages in recent humans (28, 29). (There are no available histological data on maxillary M3 initiation in recent humans or mandibular M3 initiation in Neanderthals for a more direct comparison.) We note that mandibular M3 initiation can be highly variable; radiographic evidence reveals minimum ages as early as 6 to 7 y, with ranges as large as 5 y within recent human populations (28–30). Only two histological estimates of recent human mandibular M3 initiation are available: 6.4 y of age for an African individual (31) and 7.7 y of age for a medieval European individual (32). The Le Moustier 1 age at death in this study employs the maxillary M3 initiation age from the Scladina Neanderthal to estimate death at 11.6 to 12.1 y of age (*SI Appendix*, Table S8). Although we prefer to use taxon-specific information when available, the difference between Neanderthal and recent human regression lines remains significant even when the initiation age used to calculate Le Moustier's age is increased by as much as 5 y. Thus, the finding that recent humans show significantly slower dental maturation than Neanderthals appears to be robust.

Finally, our juvenile sample indicates that Neanderthal M1 emergence likely occurred within the faster half of recent human age ranges, which average 4.7 to 7.0 y across global populations (28). Juvenile hominins at this developmental stage are extremely rare. Although the fossil individuals we studied either pre- or postdate M1 emergence at death, three Neanderthals are informative. The Krapina Maxilla B individual erupted its maxillary M1s before death at 5.9 y of age, as revealed by slight wear facets. The La Quina H18 juvenile, which is developmentally younger than Krapina Maxilla B (*SI Appendix*, Figs. S2 and S3, and Table S7), appears to have erupted its maxillary M1s even earlier, as revealed by extensive attrition on both molars and exposed dentine on the right M1. This evidence is consistent with the Scladina Neanderthal, which shows a pattern of heavy M1 attrition at 8 y of age, rapid M1 root extension, a young age of M1 root completion, and mandibular M2 emergence 2 to 5 y before recent human average ages (28). In contrast to these findings, Macchiarelli and colleagues (18) reported that M1 emergence occurred in an isolated Neanderthal tooth from La Chaise at 6.7 y of age, which is at the high end of the recent human range. However, to derive this age, the root length present at eruption was estimated from the fully formed tooth, although there are no available root length data from Neanderthals with erupting M1s. Moreover, studies of great apes show that root lengths can be quite variable as teeth emerge (33), complicating attempts to predict eruptive root lengths from fully formed teeth.

Although M1 eruption, brain mass, and body mass are broadly correlated across primates (1–3), our study does not support predictions for late age at M1 emergence in either Neanderthals or fossil *H. sapiens* (contra ref. 1). At least two of our fossil juveniles (Krapina Maxilla B, Qafzeh 10) erupted M1 earlier than many human population mean ages (28), which may also have been the case for the Scladina and La Quina H18 juveniles. The confidence intervals of the primate regression equation used to predict M1 emergence age from cranial capacity in hominins (1) has been characterized as "undesirably large" (34; also see ref. 3). Comparisons of variable traits, such as M1 eruption age, among closely related taxa may not be as illustrative as higher-level taxonomic comparisons (7), which have revealed potential "grade shifts" among broad primate groups (3). These findings underscore the need for additional research into the significance of variation in M1 eruption age within and among human populations. Moreover, future recoveries of Neanderthal and fossil *H. sapiens* juveniles who died at this key developmental stage are necessary to provide firm M1 eruption ages.

Comprehensive tooth formation data in expanded hominin samples are also of interest in a broader evolutionary context. Estimates of crown formation, molar eruption age, and/or age at death in three early *Homo* individuals (Sangiran S7-37, KNM-ER 820, KNM-WT 15000) suggest that the modern human developmental condition arose in taxa postdating *Homo erectus* (12, 16, 35, 36; also see ref. 37). Postcanine tooth development in early *Homo* appears to be accelerated relative to the anterior dentition (36), which is also apparent in the Neanderthals examined in the present study (and in ref. 30). Crown formation times estimated for a lower fourth premolar (P4) and M1 of Sangiran S7-37 are 2.7 and 2.5 y (12), respectively, which are similar to our Neanderthal P4 and M1 formation times of 2.9 and 2.6 y. Although none of the three early *Homo* individuals died while erupting their molars, Dean and colleagues have estimated respective M1 and M2 eruption ages at 4.4 and 7.6 y (12), suggesting a slightly more prolonged period of growth than in australopithecines or living apes (35, 36). Whereas it is unlikely that Neanderthals routinely erupted their M1s as early as 4.4 y of age, the M2s of Scladina had emerged before death at 8 y of age, which is similar to estimates for early *Homo*. Unfortunately, less is known about dental development in taxa postdating *H. erectus* and predating Neanderthals. *Homo antecessor* and *Homo heidelbergensis* long-period line (perikymata) numbers are reported to be more similar to Neanderthal anterior teeth than to modern humans (38). Assuming cuspal enamel formation times and long-period line periodicities similar to either Neanderthal or recent human mean values would yield shorter crown formation times in both *H. antecessor* and *H. heidelbergensis* than in *H. sapiens*. Un-

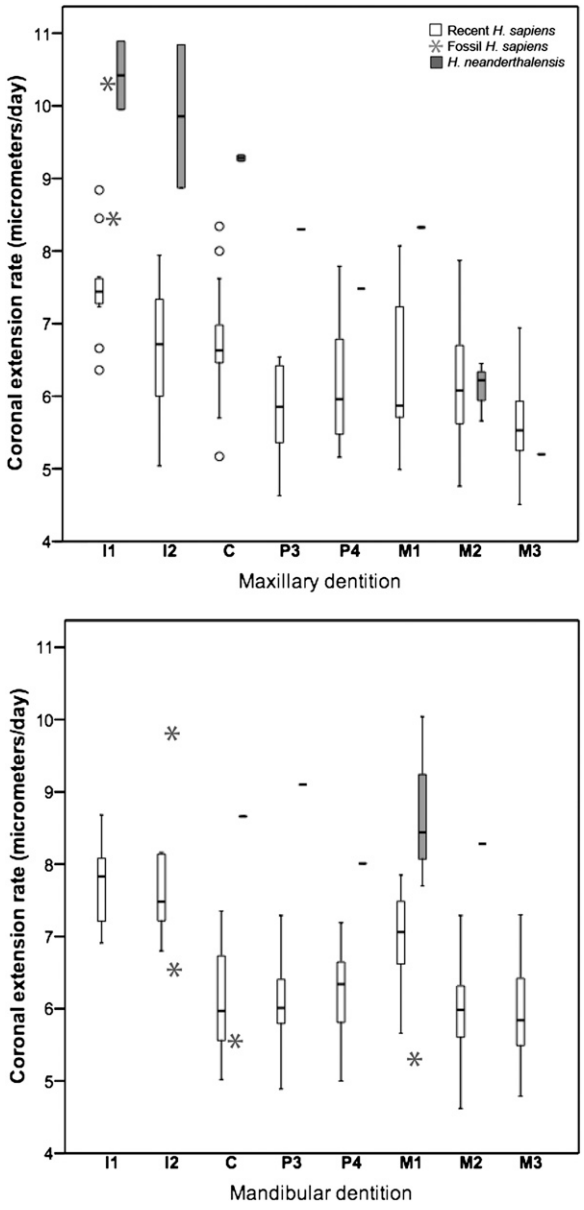

Fig. 2. Box-and-whisker plot of average coronal extension rates in recent and fossil *H. sapiens* and Neanderthals for the maxillary (*Upper*) and mandibular (*Lower*) dentitions. Postcanine teeth are represented by mesiobuccal cusps.

fortunately there are no comparable data on molar formation or eruption in either taxon; a recent report on dental development in *H. antecessor* (39) does not include any data on incremental growth in this species. In summary, although it is appears that crown formation times increased and molar eruption occurred at later ages during the evolution of *Homo*, available evidence suggests that consistently prolonged dental development may have first appeared in *H. sapiens*.

These findings provide important insight into developmental processes that are relevant to energy allocation and survival (4). Some have argued that harsh conditions created high young adult mortality rates in Neanderthals, which may have acted as a selective pressure to maintain a rapid maturation pattern (40, 41). Others have argued that risky developmental environments may favor slower growth in juvenile primates (42; but see ref. 4). It is tempting to speculate that variation in tooth formation may indicate broader life history trends, as subtle ontogenetic differences between Neanderthals and *H. sapiens* have also been reported for the cranium (43–45) and postcranium (46). Recent sequencing of the Neanderthal genome has shown that genes involved in skeletal development and cognitive abilities may also differ between these taxa (47), opening the exciting possibility of the input of comparative genomic analyses into this debate. Although additional study is necessary to assess the adaptive significance of developmental variation, absolute ages of death that are independent of reference populations are an essential first step for understanding the evolution of hominin craniodental and skeletal ontogeny (35, 48).

Materials and Methods

Virtual Imaging of Macro- and Microstructure. Overview scans of isolated teeth and those in situ were performed with laboratory microtomographic scanners (BIR Actis 300/225 FP or Skyscan 1172) with voxel sizes between 14 and 31 μm (as in refs. 13 and 14) or with synchrotron microtomography (micro-CT) on beamline ID19 of the European Synchrotron Radiation Facility with voxel sizes between 20 and 31 μm. Virtual planes of section were generated with VoxBlast Software (Vaytek, Inc.) or VG Studio MAX 2.0 (Volume Graphics, Inc.) by locating a "developmental plane" bisecting the dentine and pulpal horns in a labio-lingual or bucco-lingual orientation for anterior and postcanine teeth, respectively. These sections were used to measure cuspal enamel thickness and enamel-dentine junction length. Additional sections were cut to measure root length and assess overall tooth formation (*SI Appendix*, Figs. S2–S11), as detailed below. Phase contrast synchrotron scans were performed for certain specimens with long propagation distances (4–6 m) and voxel sizes of 7.45 or 4.95 μm (at 51 or 60 keV) to visualize long-period lines in enamel and dentine (Fig. 1 and Movie S1). Selected areas were scanned with 0.7-μm voxel size in local phase contrast or holotomography mode (at 52 keV) to quantify fine incremental features in 10 of 11 juveniles (following refs. 14 and 20). It was not possible to transport the Obi-Rakhmat 1 individual for virtual imaging. For certain samples, an additional phase retrieval process (49, 50) was used to improve reconstructed data quality for single-distance scans or multiple-distance scans (holotomography) before virtual sectioning.

Crown Formation, Root Formation, and Age at Death. Crown formation time was calculated from measurements of cuspal enamel thickness and incremental features in enamel (as summed cuspal and lateral formation times). Cuspal enamel thickness was measured from the dentine horn tip to the approximate position of the first-formed long-period line (perikyma) at the crown surface. Cuspal enamel formation time was calculated as an average of two methods (results of each typically differ by 1–2 mo). For recent and fossil *H. sapiens*, a minimum value was determined as cuspal enamel thickness divided by average daily secretion rate values of 3.80 and 4.11 μm/d for anterior and postcanine teeth, respectively (as in ref. 14). For Neanderthals, cuspal enamel thickness was divided by an average cuspal daily secretion rate of 3.84 μm/d, measured from the Lakonis Neanderthal M3 (24). Maximum cuspal formation time was determined as the minimum time multiplied by a correction factor of 1.15 to compensate for 3D prism deviation (decussation) (51). Lateral enamel formation time was calculated by multiplying the number of long-period lines (Retzius lines or perikymata) by the long-period line periodicity. High-resolution impressions and casts were produced to quantify long-period lines (on crowns and roots, as in refs. 13 and 14), which were counted on unworn or lightly worn crowns using stereomicroscopy at a magnification of 40 to 50×. Long-period line periodicities for most juvenile specimens were observed with 0.7-μm phase contrast scans (*SI Appendix*, Figs. S12 and S13), except the Scladina individual, which was physically-sectioned (13) and later confirmed with synchrotron imaging. Crown formation time estimates for the Obi Rakhmat 1 individual were used for age-at-death calculation only (detailed below). Coronal extension rates were calculated by dividing the cusp-specific enamel-dentine junction length by the respective crown formation time.

Our recent human comparative sample includes European, North American, and African physically-sectioned teeth (27, 52, 53); available material was screened to select unworn and lightly worn teeth cut nonobliquely (equivalent to the degree of wear and section orientation in our fossil sample). Comparative sample sizes are thus reduced relative to original publications as a result of these criteria. Developmental variables were calculated as detailed for fossil samples. Despite the potential for overestimation of linear enamel thickness from physically-sectioned teeth, mean values for our recent human molar sample were within one SD of virtually-sectioned recent human molars (54) for 11 of 12 cusp-specific comparisons. There was no trend for cuspal enamel thickness values from physically-sectioned teeth to exceed the mean

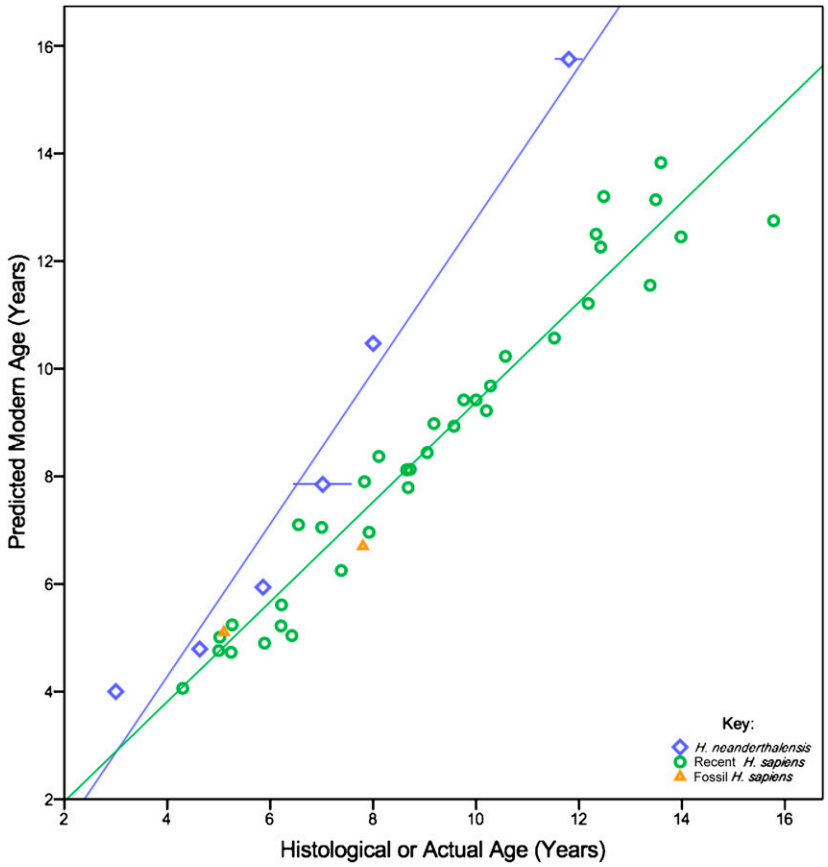

Fig. 3. Regression of predicted versus actual age for eight fossil juveniles and 36 recent (living) humans. Predicted ages are derived from human radiographic calcification standards. Fossil *H. sapiens* are represented by Qafzeh 10 and Irhoud 3; Neanderthals are represented by Engis 2, Gibraltar 2, Krapina Maxilla B, Obi-Rakhmat 1, Scladina, and Le Moustier 1 (from left to right).

values of virtually-sectioned teeth, as would be expected if section obliquity was influencing values; exactly 50% of the physically-sectioned mean values were greater than the virtually-sectioned means. Statistical tests performed with SPSS software (v. 17; SPSS Inc.) include nonparametric Mann-Whitney *U* tests for comparisons of cusp-specific enamel thickness (where $n > 3$) and long-period line periodicities between Neanderthals, recent humans, and fossil *H. sapiens*.

Root formation was assessed from counts and measurements of internal long-period (Andresen) lines in root dentine (*SI Appendix*, Fig. S14) for Engis 2, Gibraltar 2, Krapina Maxilla B, and Qafzeh 10, or from equivalent external long-period lines (periradicular bands) for Obi-Rakhmat 1, Scladina, and Irhoud 3. Long-period line number was multiplied by the long-period line periodicity to yield the time between crown completion and death in developing roots. Age at death was calculated for Engis 2, Gibraltar 2, and Scladina by identification of the neonatal (birth) line in M1s (Fig. 1 and *SI Appendix*, Fig. S1) and summation of subsequent crown and root formation times. For Krapina Maxilla B, Obi-Rakhmat 1, Le Moustier 1, Irhoud 3, and Qafzeh 10, age at death was determined as the sum of initiation age and developmental time of specific teeth (*SI Appendix*, Tables S8–S10; also see ref. 14). For Gibraltar 2, Krapina Maxilla B, and Scladina, developmental stress indicators (hypoplasias or accentuated lines) were matched between developmentally overlapping teeth, allowing temporal cross-matching across the dentition, and resulting in a continuous chronology. Initiation ages from Scladina (13) were used for Neanderthals dentitions that could not be cross-matched; a recent human initiation age was used for Irhoud 3 (32). For Qafzeh 10, the distolingual cusp of the maxillary M1 was estimated to have begun formation at birth, and a pair of hypoplasias was used to register the M1 to the maxillary central incisor (I1), which completed crown formation shortly before death. For Obi-Rakhmat 1, which was not micro-CT scanned, age at death was calculated for multiple elements as the sum of initiation age, average Neanderthal cuspal formation time, and long-period line numbers (counted on crown and root casts) multiplied by the minimum and maximum Neanderthal long-period line periodicity values (*SI Appendix*, Table S10). It was not possible to derive histological ages at death for Krapina Maxilla C, La Quina H18, or Qafzeh 15.

To compare dental ontogeny in Neanderthals, fossil *H. sapiens*, and recent humans, the overall development of each dentition was assessed through published radiographs, micro-CT slices, and isolated elements (*SI Appendix*, Figs. S2–S11, and S15). The degree of calcification of each tooth was scored several times on a developmental scale of 1 to 14, according to the system of Moorrees and colleagues (55) and Smith (56). Average scores were converted into recent human ages for each tooth using an average of male and female means in Tables 1 to 4 from ref. 26, which were averaged to yield age at death for each individual (*SI Appendix*, Table S7). We realize that micro-CT data are more precise than flat-plane radiographic data; the latter tend to overestimate crown initiation age and underestimate both crown completion and root initiation ages (57). For comparison with human radiographic data, published radiographs of the fossils were used when possible, or micro-CT images were interpreted in keeping with radiographic image bias (i.e., in a few instances crown completion and root initiation were scored at an earlier stage when the developmental stage was intermediate between two stages). Predicted recent human ages were then regressed against histological ages for each individual (Fig. 3). Median values for age ranges of Obi-Rakhmat 1 and Le Moustier 1 were used to calculate the slope of the Neanderthal linear regression line using SPSS. Our comparative sample of western European known sex and age children includes four individuals from (26) and panoramic radiographs of 32 additional individuals (scored following refs. 55 and 56). The equality of Neanderthal and recent human slopes was assessed with a nonparametric test (58) to avoid potential violations of parametric statistical assumptions.

ACKNOWLEDGMENTS. For assistance with samples and data acquisition, we thank Yoel Rak, Assaf Marom, Catherine Schwab, Michael Richards, Michael Walker, Bernard Vandermeersch, Fred Grine, Shannon McPherron, Antonio Rosas, Robert Kruszynski, Christina Verna, Patrick Semal, Michèle Morgan, Chris Dean, Robin Feeney, Heiko Temming, Andreas Winzer, Christine Verna, the Jonzac excavators, and the ID 19 beamline staff. Helpful discussions and

comments on this manuscript were provided by Chris Dean, Wendy Dirks, Jay Kelley, Karen Kramer, Dan Lieberman, Charles Nunn, and David Pilbeam. This study was funded by the Max Planck Society, the European Synchrotron Radiation Facility, and Harvard University.

1. Smith BH, Tompkins RL (1995) Toward a life history of the hominidae. *Annu Rev Anthropol* 24:257–279.
2. Smith BH (1989) Dental development as a measure of life history variation in primates. *Evolution* 43:683–688.
3. Kelley J, Smith TM (2003) Age at first molar emergence in early Miocene *Afropithecus turkanensis* and life-history evolution in the Hominoidea. *J Hum Evol* 44:307–329.
4. Godfrey LR, Samonds KE, Jungers WL, Sutherland MR (2001) Teeth, brains, and primate life histories. *Am J Phys Anthropol* 114:192–214.
5. Dirks W, Bowman JE (2007) Life history theory and dental development in four species of catarrhine primates. *J Hum Evol* 53:309–320.
6. Robson SL, Wood B (2008) Hominin life history: Reconstruction and evolution. *J Anat* 212:394–425.
7. Guatelli-Steinberg D (2009) Recent studies of dental development in Neandertals: Implications for Neandertal life histories. *Evol Anthropol* 18:9–20.
8. Leigh SR, Blomquist GE (2007) *Primates in Perspective*, eds Campbell CJ, Fuentes A, MacKinnon KC, Panger M, Bearder SK (Oxford Univ Press, Oxford), pp 396–407.
9. Bogin B (1990) The evolution of human childhood. *Bioscience* 40:1–25.
10. Kaplan H, Hill K, Lancaster J, Hurtado AM (2000) A theory of human life history evolution: Diet, intelligence, and longevity. *Evol Anthropol* 9:156–185.
11. Bock J, Sellen DW (2002) Childhood and the evolution of the human life course: An introduction. *Hum Nat* 13:153–159.
12. Dean C, et al. (2001) Growth processes in teeth distinguish modern humans from *Homo erectus* and earlier hominins. *Nature* 414:628–631.
13. Smith TM, Toussaint M, Reid DJ, Olejniczak AJ, Hublin J-J (2007) Rapid dental development in a Middle Paleolithic Belgian Neanderthal. *Proc Natl Acad Sci USA* 104: 20220–20225.
14. Smith TM, et al. (2007) Earliest evidence of modern human life history in North African early *Homo sapiens*. *Proc Natl Acad Sci USA* 104:6128–6133.
15. Smith TM (2008) Incremental dental development: Methods and applications in hominoid evolutionary studies. *J Hum Evol* 54:205–224.
16. Bromage TG, Dean MC (1985) Re-evaluation of the age at death of immature fossil hominids. *Nature* 317:525–527.
17. Lacruz RS, Ramirez Rozzi FV (2010) Molar crown development in *Australopithecus afarensis*. *J Hum Evol* 58:201–206.
18. Macchiarelli R, et al. (2006) How Neanderthal molar teeth grew. *Nature* 444:748–751.
19. Tafforeau P, et al. (2006) Applications of X-ray synchrotron microtomography for non-destructive 3D studies of paleontological specimens. *Appl Phys, A Mater Sci Process* 83:195–202.
20. Tafforeau P, Smith TM (2008) Nondestructive imaging of hominoid dental microstructure using phase contrast X-ray synchrotron microtomography. *J Hum Evol* 54:272–278.
21. Smith TM, Reid DJ, Sirianni JE (2006) The accuracy of histological assessments of dental development and age at death. *J Anat* 208:125–138.
22. Antoine D, Hillson S, Dean MC (2009) The developmental clock of dental enamel: A test for the periodicity of prism cross-striations in modern humans and an evaluation of the most likely sources of error in histological studies of this kind. *J Anat* 214:45–55.
23. Smith TM, et al. (2010) Dental development of the Taï Forest chimpanzees revisited. *J Hum Evol* 58:363–373.
24. Smith TM, et al. (2009) Brief communication: Dental development and enamel thickness in the Lakonis Neanderthal molar. *Am J Phys Anthropol* 138:112–118.
25. Guatelli-Steinberg D, Reid DJ (2008) What molars contribute to an emerging understanding of lateral enamel formation in Neandertals vs. modern humans. *J Hum Evol* 54:236–250.
26. Anderson DL, Thompson GW, Popovich F (1976) Age of attainment of mineralization stages of the permanent dentition. *J Forensic Sci* 21:191–200.
27. Reid D, Dean MC (2006) Variation in modern human enamel formation times. *J Hum Evol* 50:329–346.
28. Liversidge HM (2003) *Patterns of Growth and Development in the Genus Homo*, eds Thompson JL, Krovitz GE, Nelson AJ (Cambridge Univ Press, Cambridge), pp 73–113.
29. Liversidge H (2008) Timing of human mandibular third molar formation. *Ann Hum Biol* 35:294–321.
30. Tompkins RL (1996) Relative dental development of Upper Pleistocene hominids compared to human population variation. *Am J Phys Anthropol* 99:103–118.
31. Dean MC, Beynon AD, Reid DJ, Whittaker DK (1993) A longitudinal study of tooth growth in a single individual based on long- and short period incremental markings in dentine and enamel. *Int J Osteoarchaeol* 3:249–264.
32. Reid DJ, Beynon AD, Ramirez Rozzi FV (1998) Histological reconstruction of dental development in four individuals from a medieval site in Picardie, France. *J Hum Evol* 35:463–477.
33. Kelley J, Dean MC, Ross S (2009) *Comparative Dental Morphology*, eds Koppe T, Meyer G, Alt K (Karger Publishers, Basel), pp 128–133.
34. Smith RJ, Gannon PJ, Smith BH (1995) Ontogeny of australopithecines and early *Homo*: Evidence from cranial capacity and dental eruption. *J Hum Evol* 29:155–168.
35. Dean MC, Smith BH (2009) *The First Humans—Origin and Early Evolution of the Genus Homo*, eds Grine F, Fleagle JG, Leakey RE (Springer, New York), pp 101–120.
36. Dean MC, Lucas VS (2009) Dental and skeletal growth in early fossil hominins. *Ann Hum Biol* 36:545–561.
37. Coqueugniot H, Hublin J-J, Veillon F, Houët F, Jacob T (2004) Early brain growth in *Homo erectus* and implications for cognitive ability. *Nature* 431:299–302.
38. Ramirez Rozzi FV, Bermudez de Castro JM (2004) Surprisingly rapid growth in Neanderthals. *Nature* 428:936–939.
39. Bermudez de Castro JM, et al. (2010) New immature hominin fossil from European Lower Pleistocene shows the earliest evidence of a modern human dental development pattern. *Proc Natl Acad Sci USA* 107:11739–11744.
40. Trinkaus E (1995) Neanderthal mortality patterns. *J Arch Sci* 22:121–142.
41. Pettitt PB (2000) Neanderthal lifecycles: Developmental and social phases in the lives of the last archaics. *World Arch* 31:351–366.
42. Janson CH, van Schaik CP (1993) *Juvenile Primates*, eds Pereira ME, Fairbanks LA (Oxford University Press, New York), pp 57–76.
43. Coqueugniot H, Hublin J-J (2007) Endocranial volume and brain growth in immature Neandertals. *Period Biol* 109:379–385.
44. Ponce de León M, et al. (2008) Neanderthal brain size at birth provides insights into the evolution of human life history. *Proc Natl Acad Sci USA* 105:13764–13768.
45. Gunz P, Neubauer S, Maureille B, Hublin J-J (2010) Brain development after birth differs between Neanderthals and modern humans. *Current Bio*, in press.
46. Nelson AJ, Thompson JL (2005) *The Neandertal Adolescent Le Moustier*, ed Ullrich H (Staatliche Museen zu Berlin – Preussischer Kulturbesitz, Berlin), pp 328–338.
47. Green RE, et al. (2010) A draft sequence of the Neandertal genome. *Science* 328: 710–722.
48. Stringer CB, Dean MC, Martin RD (1990) *Primate Life History and Evolution*, ed De Rousseau CJ (Wiley-Liss, New York), pp 115–152.
49. Guigay JP, Pagot E, Cloetens P (2007) Fourier optics approach to X-ray analyser-based imaging. *Opt Commun* 270:180–188.
50. Matzke-Karasz R, Smith RJ, Symonova R, Miller CG, Tafforeau P (2009) Sexual intercourse involving giant sperm in Cretaceous ostracode. *Science* 324:1535.
51. Risnes S (1986) Enamel apposition rate and the prism periodicity in human teeth. *Scand J Dent Res* 94:394–404.
52. Smith TM, et al. (2007) *Dental Perspectives on Human Evolution: State of the Art Research in Dental Paleoanthropology*, eds Bailey SE, Hublin J-J (Springer, Dordrecht), pp 177–192.
53. Reid DJ, Guatelli-Steinberg D, Walton P (2008) Variation in modern human premolar enamel formation times: Implications for Neandertals. *J Hum Evol* 54:225–235.
54. Suwa G, Kono RT (2005) A micro-CT based study of linear enamel thickness in the mesial cusp section of human molars: Reevaluation of methodology and assessment of within-tooth, serial, and individual variation. *Anthropol Sci* 113:273–289.
55. Moorrees CFA, Fanning EA, Hunt EE (1963) Age variation of formation stages for ten permanent teeth. *J Dent Res* 42:1490–1502.
56. Smith BH (1991) *Advances in Dental Anthropology*, eds Kelley MA, Spencer Larsen C (Wiley-Liss, New York), pp 143–168.
57. Beynon AD, Clayton CB, Ramirez Rozzi FV, Reid DJ (1998) Radiographic and histological methodologies in estimating the chronology of crown development in modern humans and great apes: A review, with some applications for studies on juvenile hominids. *J Hum Evol* 35:351–370.
58. Penfield DA, Koffler SL (1986) A nonparametric K-sample test for equality of slopes. *Educ Psychol Meas* 46:537–542.